J. Astrophys. Astr. (2002) **23,** 173–183

Connecting Global to Local Parameters in Barred Galaxy Models

N. D. Caranicolas *Department of Physics, Section of Astrophysics, Astronomy and Mechanics, University of Thessaloniki, 540 06 Thessaloniki, Greece.*
e-mail: caranic@helios.astro.auth.gr

Received 2002 March 26; accepted 2002 November 14

Abstract. We present connections between global and local parameters in a realistic dynamical model, describing motion in a barred galaxy. Expanding the global model in the vicinity of a stable Lagrange point, we find the potential of a two-dimensional perturbed harmonic oscillator, which describes local motion near the centre of the global model. The frequencies of oscillations and the coefficients of the perturbing terms are not arbitrary but are connected to the mass, the angular rotation velocity, the scale length and the strength of the galactic bar. The local energy is also connected to the global energy. A comparison of the properties of orbits in the global and local potential is also made.

Key words. Galaxies: barred—orbits—global and local parameters.

1. Introduction

We consider the barred galaxy model described by the potential

$$\Phi(r,\phi) = -\frac{M_d}{(r^2+\alpha^2)^{1/2}} - \frac{M_b}{\{r^2[1+(b^2-1)\sin\phi^2]+c_b^2\}^{1/2}}, \quad (1)$$

where r, ϕ are polar coordinates. Here M_d is the mass, α is the scale length of the disk while M_b , c_b and $b > 1$ is the mass, the scale length and the strength of the bar, respectively. In the system of galactic units used in this paper, the unit of length is $1kpc$ the unit of time is 0.97746×10^8 yr and the unit of mass is $2.325 \times 10^7\, M_\odot$. The velocity and the angular velocity units are 10 km/s and 10 km/s/kpc, respectively while G is equal to unity. Our test particle is a star of mass $= 1$. Therefore, the energy unit (per unit mass) is $100\,(\mathrm{km/s})^2$. In these units the values of the parameters are $\alpha = 12$ kpc, $b = 2$, $c_b = 1.5$ kpc, $M_d = 9500$ and $M_b = 3000$. It is evident that we consider a galaxy with a massive bar.

We shall consider the case when the bar rotates clockwise at a constant angular velocity Ω_b. The corresponding Hamiltonian, which is known as the Jacobi integral, in rectangular cartesian coordinates x, y, reads

$$H_J = \frac{1}{2}(p_x^2+p_y^2)+\Phi(x,y)-\frac{1}{2}\Omega_b^2(x^2+y^2) = \frac{1}{2}(p_x^2+p_y^2)+\Phi_{\mathrm{eff}}(x,y) = E_J, \quad (2)$$

where p_x, p_y are the momenta, per unit mass, conjugate to x and y

$$\Phi_{\mathrm{eff}}(x,y) = -\frac{M_d}{\sqrt{x^2+y^2+\alpha^2}} - \frac{M_b}{\sqrt{x^2+b^2y^2+c_b^2}} - \frac{1}{2}\Omega_b^2(x^2+y^2), \quad (3)$$

is the effective potential and E_J is the numerical value of the Jacobi integral. If we expand the effective potential (3) in a Taylor series near the centre we shall find a potential describing local motion.

The aim of the present work is:

- to find connections between global and local parameters and
- to study and compare the properties of global and local motion.

In particular, we shall express the coefficients of the local potential in terms of the global physical quantities entering potential (3). A connection of the global to local energy will be also presented.

The properties of orbits in the global model are studied in section 2. In section 3 we present the local potential, the connection between the local and global parameters and the properties of the local motion. We close with a discussion and the conclusions of this work, which are presented in section 4.

2. Orbits in the global model

Figure 1 shows contours of the constant effective potential (3), when $\Omega_b = 1.25$ in the above mentioned galactic units, which is equivalent to 12.5 km/s/kpc. One observes

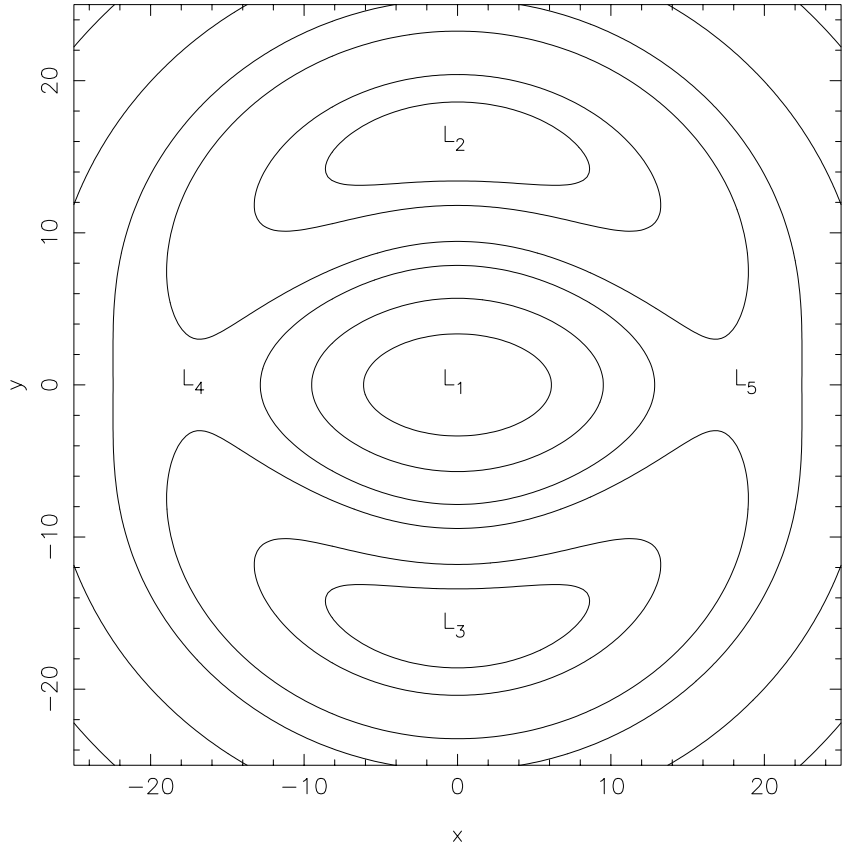

Figure 1. Contours of the constant effective potential (3) when $\Omega_b = 1.25$. The values of the parameters are $\alpha = 12$ kpc, $b = 2$, $c_b = 1.5$ kpc, $M_d = 9500$ and $M_b = 3000$. One observes that there are five stationary points marked L_1 to L_5.

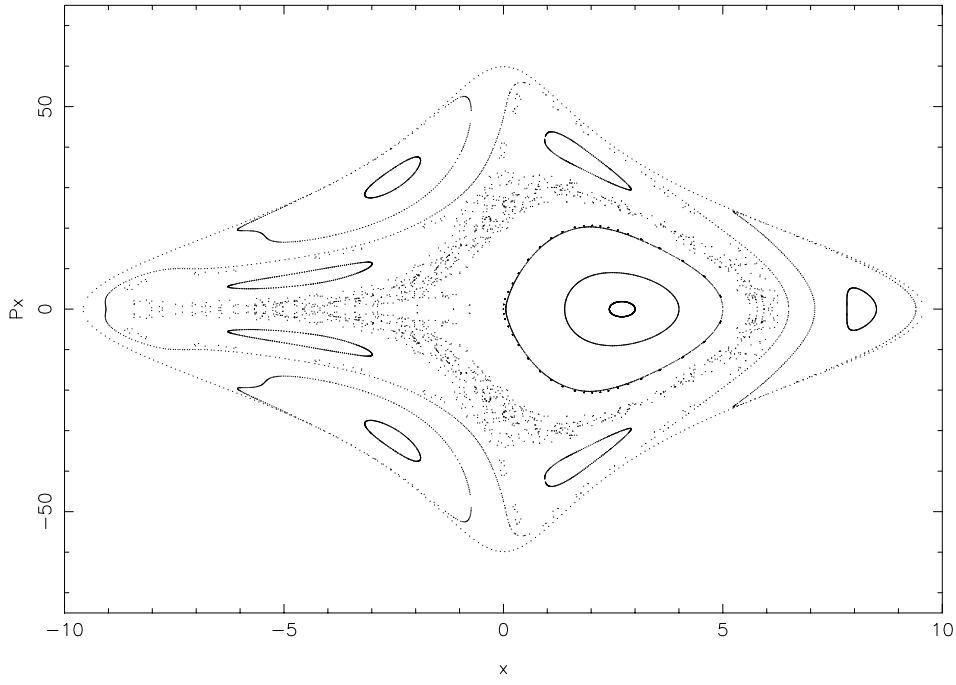

Figure 2. The $x - p_x$ phase plane for the global Hamiltonian (2) when $E_J = -1000$. The values of the parameters are as in Fig. 1.

that there are five stationary points, marked L_1 to L_5, at which

$$\frac{\partial \Phi_{\text{eff}}}{\partial x} = 0 \, , \quad \frac{\partial \Phi_{\text{eff}}}{\partial y} = 0. \tag{4}$$

These points are called "Lagrange points". The central stationary point L_1 is a minimum of Φ_{eff}. In the other four points L_2, L_3, L_4, L_5 it is possible, for the test particle, to travel in a circular orbit while appearing to be stationary in the rotating frame. For this orbit the centrifugal and gravitational force precisely balance. The stationary points L_4, L_5 on the x-axis are saddle points while L_2, L_4 are maxima of the effective potential. The annulus bounded by the circles through L_2, L_3 and L_4, L_5 is known as the "region of corotation" (see Binney & Tremaine 1987). It is important to note that the region of corotation is located somewhere at the end of the galaxy described by the model (3).

We now proceed to study the properties of orbits in the potential (3). Orbits are found by integrating numerically the equations of motion

$$\ddot{x} = -2\Omega_b \dot{y} - \frac{\partial \Phi_{\text{eff}}}{\partial x}, \quad \ddot{y} = 2\Omega_b \dot{x} - \frac{\partial \Phi_{\text{eff}}}{\partial y}, \tag{5}$$

where the dot indicates derivative with respect to the time.

In order to visualise the properties of motion we use the $x - p_x$, $y = 0$, $p_y \geq 0$ Poincare phase plane of the Hamiltonians (2). The results for $E_J = -1000$ are shown in Fig. 2. There are regular orbits, forming the nearly circular invariant curves, as well

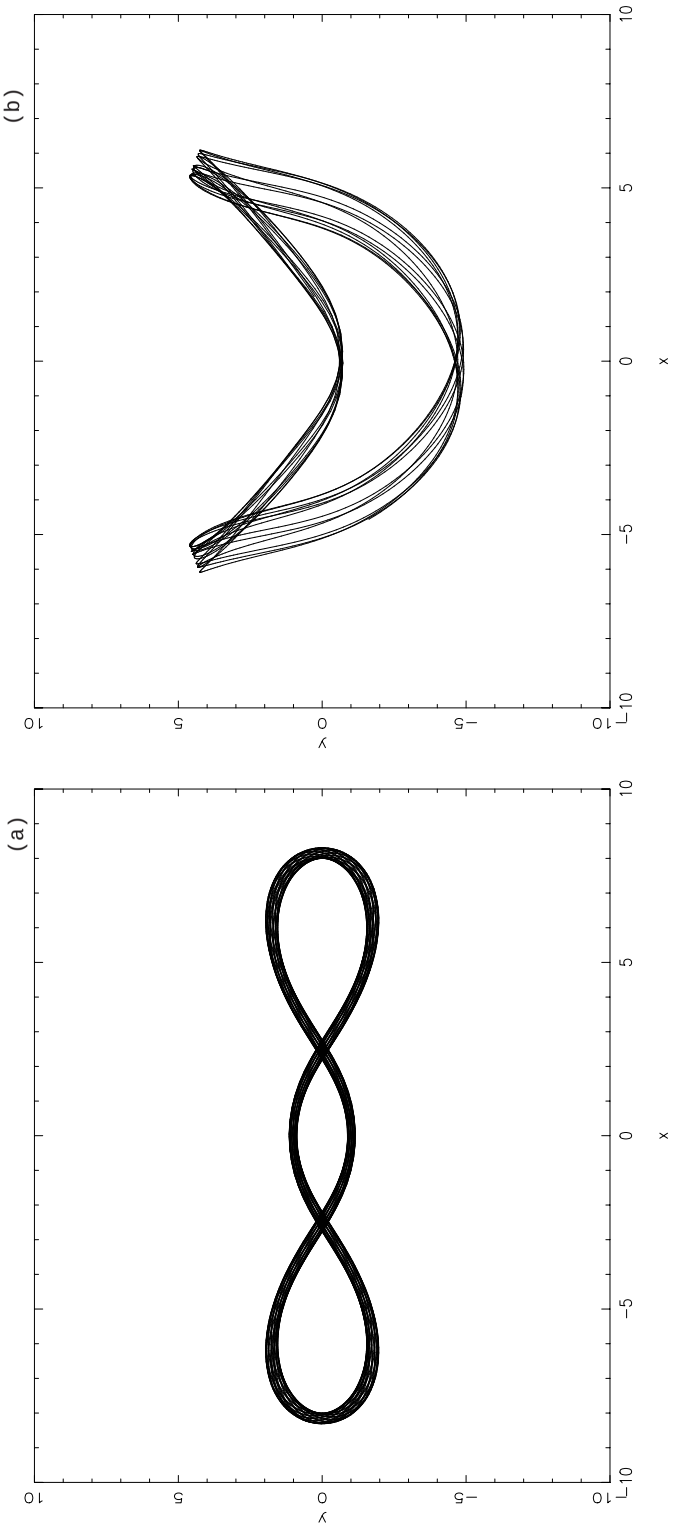

Figure 3. (*Continued*)

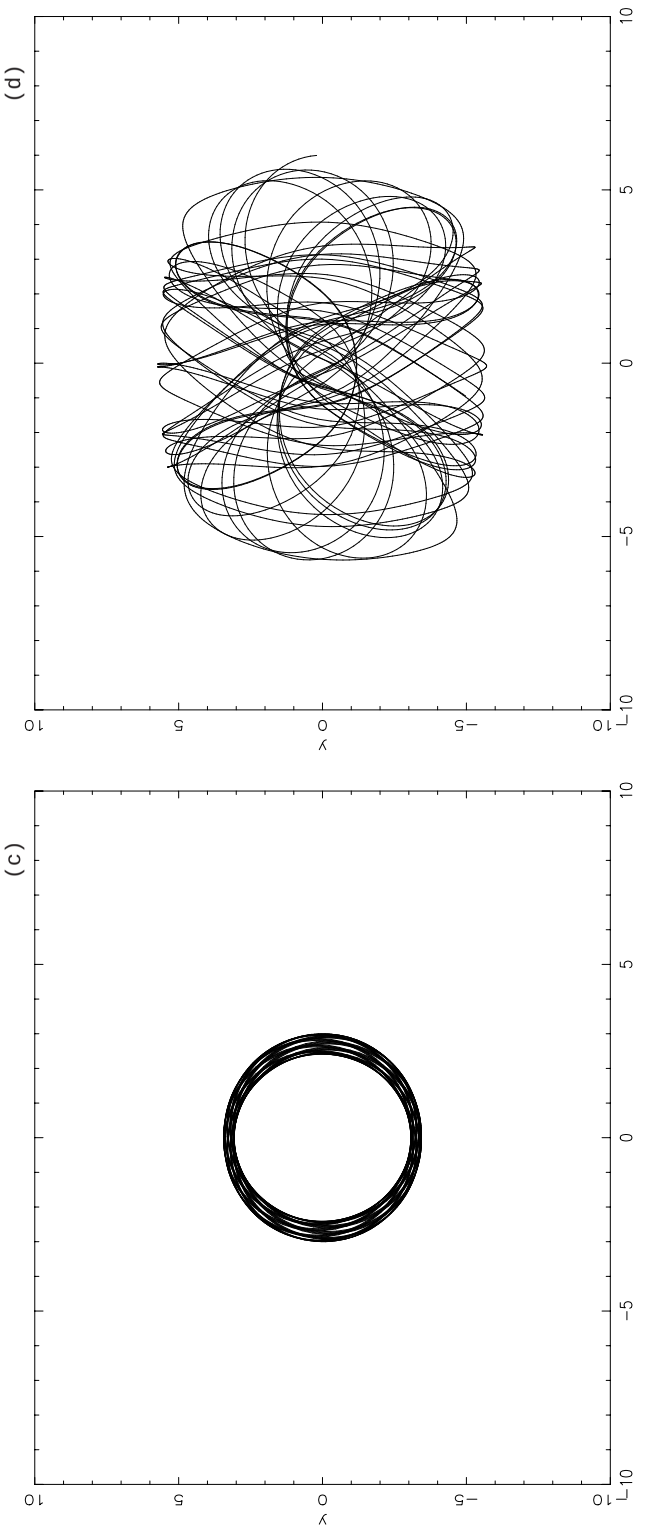

Figure 3(a–d). Orbits in the global Hamiltonian (2).The values of parameters are as in Fig. 2.

as sets of islands and chaotic orbits producing a chaotic region. The outermost curve is the limiting curve defined by the equation

$$\frac{1}{2}p_x^2 + \Phi_{\rm eff}(x) = E_J. \tag{6}$$

Figure 3(a–d) shows four typical orbits. The orbits shown in Fig. 3(a) produce the set of the three outer islands. It is evident that those elongated orbits support the bar. The orbit shown in Fig. 3(b) produces two of the inner islands while the orbit given in Fig. 3(c) produces the central invariant curves that are topologically circles. The chaotic region are produced by the orbit shown in Fig. 3(d). It is clear that the three last types of orbits support the disk. It is important to note that for the values of the parameters used, chaotic motion is present only when $c_b < 1.7$ kpc while for $c_b = 1.7$ kpc the chaotic region is negligible (see Caranicolas & Innanen 1991).

For small values of the energy the phase plane is quite different. Fig. 4 shows the $x - p_x$ phase plane when $E_J = -2700$. It is evident that, here, we have motion taking place near the stable Lagrange point L_1. The motion is regular and one observes only one kind of invariant curves. The invariant curves are topological circles closing around one unique invariant point. The corresponding orbits are box-orbits. Those forming the outer invariant curves belong to elongated boxes that support the bar while, as we approach the "central" invariant point, the boxes become more rectangular.

3. Orbits in the local potential

The local potential can be found by expanding the effective potential (3) in a Mc-Laurin series near the stable Lagrange point L_1, which coincides with the origin. Doing so,

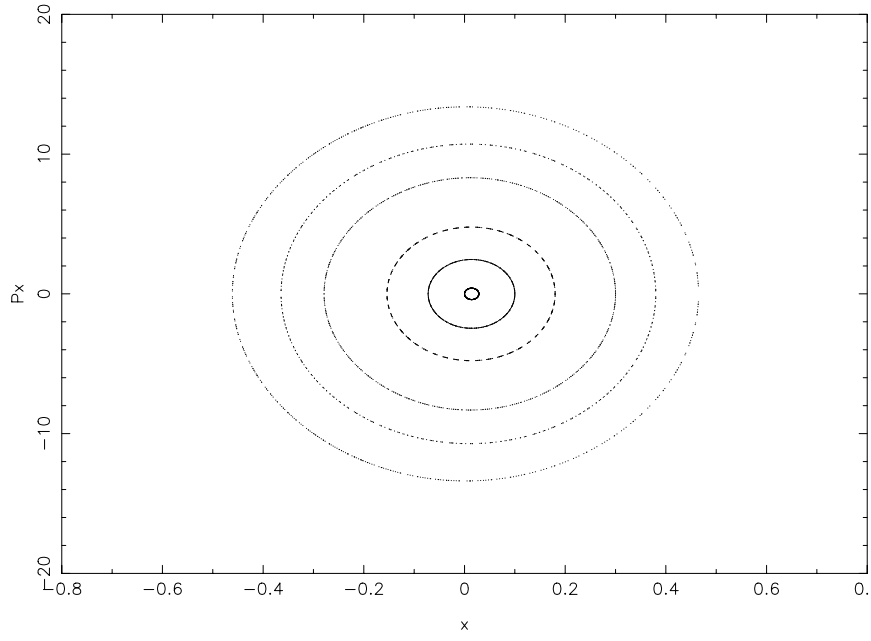

Figure 4. Same as Fig. 2 when $E_J = -2700$.

we obtain the local effective potential which reads

$$\begin{aligned} U_{\text{eff}}(\Delta x, \Delta y) = U_{\text{eff}}(0,0) &+ \frac{1}{2}A(\Delta x)^2 + \frac{1}{2}B(\Delta y)^2 \\ &- \frac{3}{8}[\alpha_1(\Delta x)^4 + 2\alpha_2(\Delta x)^2(\Delta y)^2 + \alpha_3(\Delta y)^4] \\ &- \Omega_0^2[(\Delta x)^2 + (\Delta y)^2]/2, \end{aligned} \tag{7}$$

where we have set

$$U_{\text{eff}} = \frac{\alpha}{M_d}\Phi_{\text{eff}}, \tag{8}$$

in order to avoid large numbers. Writing, for convenience, $x = \Delta x$, $y = \Delta y$, $V_{\text{eff}} = U_{\text{eff}}(x, y) - U_{\text{eff}}(0, 0)$, equation (7) becomes

$$V_{\text{eff}} = \frac{1}{2}Ax^2 + \frac{1}{2}By^2 - \frac{3}{8}[\alpha_1 x^4 + 2\alpha_2 x^2 y^2 + \alpha_3 y^4] - \Omega_0^2(x^2 + y^2)/2, \tag{9}$$

where

$$\begin{aligned} A &= \frac{1}{\alpha^2} + \frac{\alpha M_b}{M_d c_b^3}\ ,\ B = \frac{1}{\alpha^2} + \frac{\alpha b^2 M_b}{M_d c_b^3}\ ,\ \alpha_1 = \frac{1}{\alpha^4} + \frac{\alpha M_b}{M_d c_b^5}, \\ \alpha_2 &= \frac{1}{\alpha^4} + \frac{\alpha b^2 M_b}{M_d c_b^5}\ ,\ \alpha_3 = \frac{1}{\alpha^4} + \frac{\alpha b^4 M_b}{M_d c_b^5}\ ,\ \Omega_0^2 = \frac{\alpha \Omega_b^2}{M_d}. \end{aligned} \tag{10}$$

One observes, from equation (10), that the coefficients of the local effective potential are functions of the physical quantities entering the global effective potential.

The local Hamiltonian is

$$H_L = \frac{1}{2}(X^2 + Y^2) + V_{\text{eff}}(x, y) = h_L, \tag{11}$$

where X, Y are the local momenta, per unit mass, conjugate to x and y while h_L is the numerical value of the local energy. We now come to connect the global energy E_J to the local energy h_L. Note that $E_{J0} = \Phi_{\text{eff}}(0, 0)$ defines a point in the (x, y) plane while $E_J = \Phi_{\text{eff}}(x, y)$ defines a curve in the same plane. The global motion takes place inside this curve which is known as the zero velocity curve. At the same time $h_{L0} = V_{\text{eff}}(0, 0)$ defines a point in the (x, y) plane while $h_L = U_{\text{eff}}(x, y)$ defines a curve inside which the local motion takes place. This second curve is the local zero velocity curve. We consider only bounded motion, that is the zero velocity curves are always closed curves. The local energy h_L is connected to the global energy through the relation

$$\begin{aligned} h_L = U_{\text{eff}}(x, y) - U_{\text{eff}}(0, 0) &= \frac{\alpha}{M_d}[\Phi_{\text{eff}}(x, y) - \Phi_{\text{eff}}(0, 0)] \\ &= \frac{\alpha}{M_d}(E_J - E_{J0}). \end{aligned} \tag{12}$$

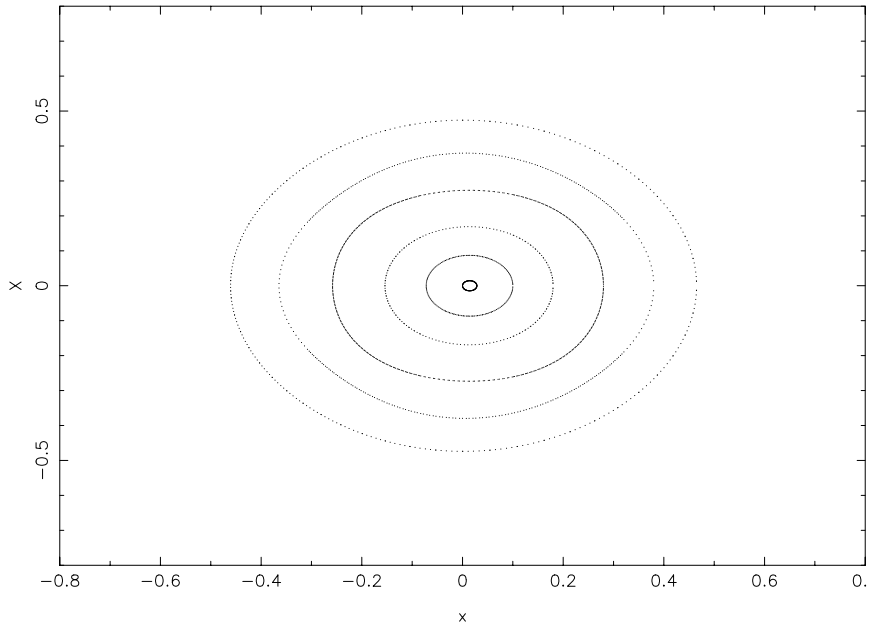

Figure 5. The $x - X$ phase plane for the local Hamiltonian (11) when $h = h_L = 0.11578$.

We now come to study the properties of local motion. For the adopted values of the global parameters and $\Omega_b = 1.25$, we find $A = 1.13$, $B = 4.50, \alpha_1 = 0.50, \alpha_2 = 2.00$, $\alpha_3 = 7.98$, $\Omega_0 = 0.044$. Using the value $E_J = -2700$ we find $h_L = 0.11578$. Fig. 5 shows the $x - X$ ($y = 0$, $Y > 0$) phase plane for the local motion. The motion is regular and one observes invariant curves that are topologically circles closing around a "central" invariant point. It is clear, that no resonant orbits are present although the ratio of the unperturbed frequencies is a rational number, namely $A^{1/2}/B^{1/2} = 1/2$. As the similarity between Figs 4 and 5 is obvious one can say that the behaviour of orbits in the local system Hamiltonian (11) is similar to that of orbits in the global Hamiltonian (2).

Figure 6 shows the $x - X$ phase plane for the local motion when $h = 0.36 > h_L$. Here things look quite different. In addition to the invariant curves closing around the "central" invariant point, one observes four sets of islands. These islands are produced by quasi periodic orbits starting near the corresponding stable periodic orbits. These periodic orbits are the well known figure-eight periodic orbits. We shall come to this point later in this section.

It is natural for the reader to ask: why for this value of local energy the properties of orbits of the local system are different from those of the corresponding global potential? The answer is the following: The expansion (9) is valid only when

$$\frac{x^2 + b^2 y^2}{c_b^2} << 1. \tag{13}$$

When $h_L = 0.11578$ we have $x \leq x_{\max} = 0.47$, $y \leq y_{\max} = 0.23$. For the above values of x and y (13) is always true when $b = 2$, $c_b = 1.5$ kpc. On the other hand, if one chooses $h = 0.36$, then $x \leq x_{\max} = 0.95$, $y \leq y_{\max} = 0.48$ and relation (13) is not valid for the same values of b and c_b. Therefore, it is obvious that the properties of

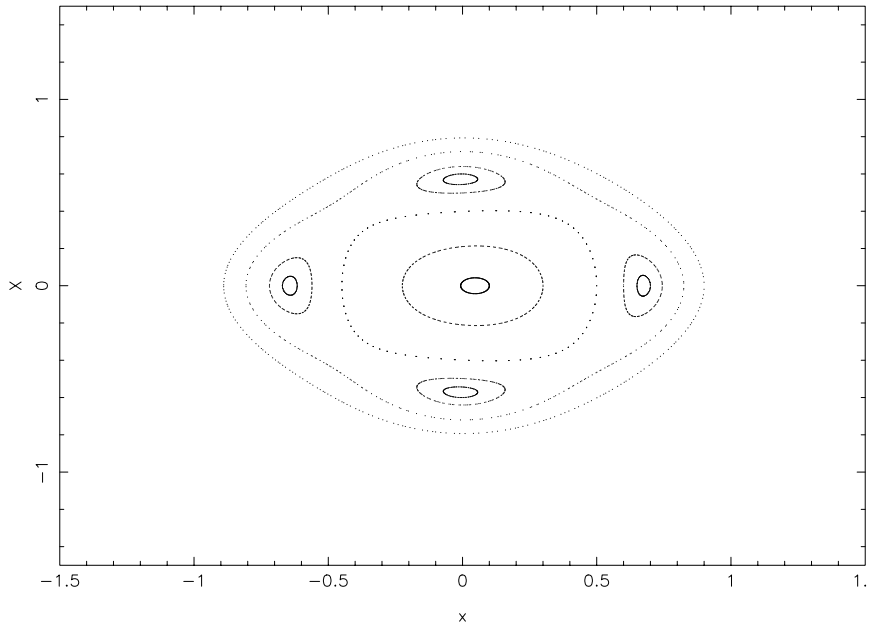

Figure 6. Same as Fig. 5 when $h = 0.36$.

orbits in the local system are the same to the properties of orbits, in the global system, only when the local energy is small enough such as relation (13) to hold. If we increase the value of energy then resonant periodic orbits appear. These orbits are stable figure-eight orbits. Near these orbits start the figure-eight quasi periodic loop orbits, which support the bar structure in the central parts of the galaxy.

It is also important to note that, for a given value of global energy, there corresponds a value of local energy through relation (12). It is obvious that this local energy does not have a meaning, if relation (13) is not satisfied. In order to observe the resonant figure-eight orbits, one must use larger values of energy for the local potential. Numerical experiments suggest that the figure-eight orbits appear for values of h about twice as large as h_L. On the other hand we must emphasise that the chaotic regions, if any, are negligible. Indeed we made many numerical calculations for energies up to the energy of escape in the local potential. Our numerical calculations have shown that the area of the phase plane covered by the quasi periodic figure-eight orbits increases while no chaotic phenomena were observed. The energy of escape for the local potential (see Caranicolas & Varvoglis 1984) is given by the relation

$$h_{\rm esc} = \frac{(B - \Omega_b^2)^2}{6\alpha_3}. \tag{14}$$

Note that, because we always study bounded motion, we must have $h_L \leq h \leq h_{\rm esc}$.

4. Discussion

During the last decades a large number of papers have been devoted to the study of dynamics of barred galaxies (see e.g. Freeman 1966; Zang & Hohl 1978; Miwa &

Noguchi 1981; Toomre 1981; Carnevali 1983; Papayannopoulos & Petrou 1983; Petrou 1984; Sparke & Sellwood 1987; Combes *et al.* 1990; Sundin & Sandelius 1991).

In the present work we have tried to find connections between the parameters of a model describing global motion in a barred galaxy and the corresponding parameters of the local potential. The local potential comes by expanding the global effective potential near the centre of the galaxy. It was shown that the local parameters and the corresponding local energy are functions of the global parameters and the global energy.

Numerical calculations in the global model suggest that, in addition to the regular orbits, there is a significant part of orbits that is chaotic. It was observed that chaotic orbits to appear need small values of the scale length of the bar. For small values of the global energy the motion is regular and all orbits are box orbits. The same is true for the local motion when relation (13) is satisfied. In other words, the properties of global and local motion are similar for small values of the global energy, which consequently give, through (12), small values for the local energy h_L.

Furthermore, we must note that in the global model the resonant orbits of type *b* as well as the chaotic orbits of type *d* carry stars in the central parts of the galaxy. Therefore we have an increasing density near L_1. It is interesting to observe that a large number of high energy stars passing near L_1 are in chaotic orbits. The other two types of orbits a and b do not contribute in the central density.

Increasing the value of energy in the local model gives rise to resonant figure-eight orbits. The present and previously derived results support the idea that these orbits seem to be important for the local barred galaxy models. With the term local barred galaxy models we mean those that are made from perturbed harmonic oscillators. The following reasons make these orbits important for galactic bars:

- It is evident that the figure-eight orbits support the barred structure.
- Starting from the figure-eight orbits and using the theory of the Inverse Problem, one can construct a local potential based on perturbed harmonic oscillators which reproduce the above orbits (see Caranicolas 1998; Caranicolas & Karanis 1998).
- Figure-eight orbits were observed not only in self consistent models (Miller & Smith 1979) but also in the present local model which comes from the realistic potential (1).

It is also important to notice that the figure-eight orbits appear for values of the energy h much more larger than the local energy h_L. Looking this fact from a physical point of view, one can say that the figure-eight orbits can be considered as a product of a particular activity near the centre of barred galaxies.

Acknowledgement

The author would like to thank an anonymous referee for useful comments.

References

Binney, J., Tremaine, Sc. 1987, *Galactic Dynamics*, (Princeton, New Jersey: Princeton University press)
Caranicolas, N. D., Varvoglis, Ch. 1984, *Astron. Astrophys.* **141**, 383.
Caranicolas, N. D., 1998, *Astron. Astrophys.* **332**, 88.
Caranicolas, N. D., Karanis, G.I. 1998, *A& SS* **259**, 45.

Caranicolas, N. D., Innanen, K.A. 1991, *A.J.* **102**, 1343.
Carnevali, P. 1983, *Ap. J.* **265**, 701.
Combes, F., Dupraz, C., Cerin, M. 1990, In: *Dynamics and Interactions of Galaxies*, (ed.) R Wielen (Berlin: Springer) p. 205
Freeman, K.C. 1966, *MNRAS* **134**, 15.
Miller, R., Smith, B.F. 1979, *Ap. J.* **227**, 785.
Miwa, T., Nochuchi, M. 1998, *Ap. J.* **499**, 149.
Papayannopoulos, Th., Petrou, M. 1983, *Astron. Astrophys.* **119**, 21.
Petrou, M. 1984, *MNRAS* **211**, 283.
Sundin, M., Sundelius, B. 1991, *Astron. Astrophys.* **245**, L5.
Sparke, S.L. , Sellwood, J.A. 1987, *MNRAS* **225**, 653.
Toomre, A. 1981, In: *The Structure and Evolution of Normal Galaxies*, (eds) S. M. Fall, I. Lyndell-Bell, (Cambridge University Press)
Zang, T.A., Hohl, F. 1978, *Ap.J.* **226**, 521.